Title

Digitalization of Human Operations in the Age of Cyber Manufacturing: Sensorimotor Analysis of Manual Grinding Performance

Permalink

Journal

ISSN

Authors

Bales, Gregory L
Das, Jayanti
Tsugawa, Jason
et al.

Publication Date

DOI

Peer reviewed

Digitalization of Human Operations in the Age of Cyber-Manufacturing: Sensorimotor Analysis of Manual Grinding Performance

Gregory L. Bales
Mechanical & Aerospace Eng.
University of California
Davis, California 95616
glbales@ucdavis.edu
ASME Member

Jayanti Das
Mechanical & Aerospace Eng.
University of California
Davis, California 95616
jydas@ucdavis.edu

Jason Tsugawa
Mechanical & Aerospace Eng.
University of California
Davis, California 95616
jztsugawa@ucdavis.edu

Barbara Linke
Mechanical & Aerospace Eng.
University of California
Davis, California 95616
bslinke@ucdavis.edu
ASME Member

Zhaodan Kong
Mechanical & Aerospace Eng.
University of California
Davis, California 95616
zdkong@ucdavis.edu
ASME Member

This paper presents new techniques to analyze and understand the sensorimotor characteristics of manual operations such as grinding, and links their influence on process performance. A grinding task, though simple, requires the practitioner to combine elements from the large repertoire of his or her skillset. Based on the joint gaze, force, and velocity data collected from a series of manual grinding experiments, we have compared operators with different levels of experience and quantitatively described characteristics of human manual skill and their effects on manufacturing process parameters such as cutting energy, surface finish, and material removal rate. For instance, we find that an experienced subject performs the task in a precise manner by moving the tool in complex paths, with lower applied forces and velocities, and short fixations compared to a novice. A detailed understanding of gaze-motor behavior broadens our knowledge of how a manual task is executed. Our results help to provide this extra insight, and impact future efforts in workforce training as well as the digitalization of manual expertise, thereby facilitating the transformation of raw data into product-specific knowledge.

1 Introduction

In the age of cyber-manufacturing, research has increasingly focused on establishing intelligent processes which will enable the effective communication between humans, machines, and products in complex production environments. Within this new infrastructure, an understanding of human performance is critical if they are directly involved in product generation. For example, the quality of manual abrasive finishing operations such as grinding, polishing, and engraving are heavily dependent upon the performance of the individual operator. These manual sectors represent a growing market, from foundry shops to the aerospace industry. The skills involved in these manual tasks are largely procedural rather than declarative, meaning that they cannot be easily articulated by the individuals [10]. Furthermore, a lack of understanding of these manual skills may prolong the transfer of this knowledge from one generation to the next. It may also impede the development of efficient collaboration between humans and smart machines [26] which can greatly impact the product outcome [9, 16]. If we wish to integrate humans into the manufacturing network and effectively train them, we need to digitalize their behavior/performance. A first step in this process is the development of a formal mod-

els which capture the process properties, behavioral characteristics and techniques of the practitioners. Such models would allow the optimization and integration between person to person, person to machine, and person to tool within the manufacturing network [25].

A crucial issue for manual grinding operation is a critical understanding of fundamental cutting mechanisms. Manual grinding operations are effectively force controlled processes rather than automated path controlled operations. The applied forces are influenced by several factors, which include the gripping force of the user, personal skill level, and cutting tool feed rate [4]. Extensive research has focused on different automated grinding processes and has characterized the influence of process control parameters such as material removal rate, grinding force, wheel structure topography, etc. [13, 18]. Unfortunately, very little work has been carried out to investigate manual grinding operations and process optimization, and to correlate the experience level of the worker to asses process performance quality. Kyle et al. [21] described the input-output streams of a manual grinding process, reviewed sustainability aspects of the energy sources of abrasive power and grinding tools, and discussed concerns related to the safety and health aspects of manual operations. Along with other process parameters such as feed rate, cutting speed, and workpiece materials, the skill level of the practitioner plays a critical role in product performance and process optimization.

It has been stated that the resultant tangential and normal forces from manual grinding operations have an impact on process parameters such as material removal rate (MRR), surface integrity (e.g. average roughness), and control process performance [5]. Thus the efficiency of manual grinding operations are largely dependent on judicious control of applied forces and become a function of the experience level of the practitioner, MRR, average roughness etc. However, little work has been done to investigate the impact of manual grinding forces on process performance (i.e. in terms of MRR and surface roughness) based on experience level. We shall explore the performance of manual grinding operations by examining normal and tangential forces, the experience of the user, material removal rate, and surface integrity in addition to visual-attention-motor behavior.

Visual attention is a remarkable human capability of reducing the huge amount of visual data entering our eyes into a manageable level. It can be roughly divided into two categories, bottom-up attention and top-down attention [2, 22]. Top-down or voluntary attention is our ability to intentionally attend to an external stimulus. It is a goal-driven process based on aspects such as tasks, knowledge, expectations, and memory. In a manual grinding scenario, for instance, it may involve finding a sample. Bottom-up or reflexive attention is a stimulus-driven process in which a salient sensory event captures our attention. Such an event might be a crack appearing on the surface of the grinding sample. It is widely accepted that visual attention is not decoupled from motor system in natural behavior [8, 15, 24, 27]. In the majority of studies concerned with visual attention and the motor system, actions are discrete, e.g., "remove the lid of the kettle"

and "select a peanut butter jar" [15, 27], and manually labeled by humans. Such a representation fails to capture the complex nature of gaze-motor behavior. Data on motor dynamics, such as the changes in forces, were not collected and subsequently studied. A analysis that captures the dynamic nature of motor behavior is needed, similar to those developed in [14, 17].

This paper studies the visual-attention-motor behavioral characteristics involved in a manual grinding task and examines their effect on performance and surface integrity. The primary goal of our effort is to gain knowledge that would aid in the development of a smart, analytic system for manual grinding operations that can transform experienced-based knowledge into quantitative data. This system will aid in improving human-machine interactions and can be used to collect and transform raw data into product-specific knowledge to develop a globally modeled platform. Our study, on the one hand, improves our understanding of complex manual skills that are beyond our everyday activities and, on the other hand, enables models of human skills which are crucial for building future industrial robots that can understand human intentions.

The contribution of the paper is two fold. First, we quantitatively characterize manual behaviors by comparing joint gaze-motor data. To our knowledge, this paper is one of the first instances in which visual attention has been studied in manufacturing scenarios. Second, we examine the relationships between applied grinding forces and surface integrity with respect to these behaviors, and the experience level of the practitioner. We are able to show that there are distinct behavioral and performance differences between subjects of different experience levels. Adept hand eye coordination is key to the performance of a number of manufacturing processes. Due to the importance of gaze-motor behavior, our results can be generalized to gain insight into a wide range of industrial activities such as welding, repairing machinery, grinding and polishing during abrasive finishing process, or everyday activities like driving.

The paper is organized as follows: in Section 2, we discuss the details of the experiment, including the setup and procedure. In Section 3, we discuss our data processing methods. Section 4 presents our results along with a discussion. We conclude the paper in Section 5.

2 Experiment

In this section, we describe the setup and procedure of our manual grinding experiment.

2.1 Setup

For the purpose of studying manual skills involved in grinding tasks, we recruited four students from the Department of Mechanical and Aerospace Engineering at the University of California, Davis. All subjects were between 20 to 25 years of age. The subjects were chosen based on their differing levels of experience. For this study we have subjectively defined experience as the amount of time each subject

has spent with grinding tools. In the subsequent sections, the "experienced" subject shall be referred to as Subject 1, the "intermediate" subjects as Subject 2 and Subject 3, and the "novice" subject as Subject 4. Each subject performed ten trials in which they were asked to use an abrasive wheel to grind a metal sample. As shown in Figure 1, three streams of data were collected. First, we measured the direction of gaze with a head mounted eye tracking system. Second, the grinding forces were measured with a triaxial load cell mounted beneath the grinding sample. Lastly, the 6 DOF kinematic state of the grinding tool and the eye tracking glasses were recorded using an optical motion tracking system.

We measured gaze using a wearable eye tracking system manufactured by SensoMotoric Instruments (SMI). The SMI ETG 2w system is integrated into a set of glasses which can extract binocular gaze, while simultaneously recording a video of the visual point of view. Pupil images and corneal reflection points are used to determine the vertical and horizontal angular orientation of each individual eye, which in turn are used to calculate the gaze. True gaze direction requires a vector to describe its full nature. In our analysis, the gaze data were represented as a binocular points of regard (BPOR). These points describe where the binocular gaze vector pierces the gaze plane, a hypothetical projection plane located 1450 mm in front of the glasses. The BPOR were sampled at 60 Hz, and the gaze was presented as their pixel positions within the video image. Videos were recorded at 60 frames per second at a resolution of 1280 pixels horizontally and 960 pixels vertically.

The material used in this study was 6061 aluminum in the form of test coupons with dimensions of 5.0 cm in length, by 2.5 cm in width, by 2.5 cm in height. Each grinding experiment was conducted with a Dremel 4000 hand held power tool using alumina sanding bands of 60 grit sizes (mesh number). The power tool was running at a constant speed of 5000 rpm. All grinding operations were performed under dry cutting conditions. The grinding force was varied manually which produced force variations in the tangential, normal, and axial directions as shown in Figure 2. A piezo-electric transducer based load cell (Kistler 9252A) was mounted under the workpiece to measure these grinding forces during machining. A vise was used to fasten the workpiece to the sensor. Force data were sampled at 1000 Hz using a National Instruments DAQ and Labview software.

Finally, we obtained the kinematic data using a motion capture system by Optitrack. This system consists of twelve cameras mounted circumferentially along the walls of our lab. These camera modules each contain a ring of infrared light emitting diodes which project a cone of IR light into the lab space. The eye tracking glasses, and the grinding tool were each defined as a rigid body by marking them with a series of reflective spheres as shown in Figure 2. The overlap of the IR cones establish a tracking volume in which the position of these markers are determined at <1mm accuracy. From these marker positions, the Optitrack software can extract the 6 DOF pose estimation of each rigid body. Data was sampled at 120Hz.

2.2 Procedure
The experiment proceeded in the following manner:

1. Before each grinding trial, a calibration step was carried out in order to collect the particular ocular behaviors of the subject using a method is described in [1].
2. Light touched crosshatched marks were made on top of workpiece surfaces. The subjects were asked to grind the surfaces until the marks were no longer visible.
3. The gaze, force, and kinematic data were collected and saved separately for each trial, and each subject.
4. Both the grinding wheel and the grinding sample were replaced after each trial.
5. The mass of the sample was recorded before and after each grinding trial to determine the amount of the mass removed.
6. Average surface roughness was measured and recorded.
7. Each subject performed ten trials.

3 Data Processing Methods
In this section we describe our basic data processing methods.

3.1 Time Alignment and Filtering
All data from the three individual streams had to be temporally aligned, buffered, and filtered for a comparative analysis. The data analysis was performed in Matlab.

The force and kinematic data were post-processed with a 8th order Butterworth low pass filter at a corner frequency of 20Hz. Normal and axial force data were particularly noisy necessitating the use of such an aggressive filter to extract characteristics at the lower frequencies. Filtering was accomplished using a bidirectional, zero lag implementation of digital filters.

3.2 Scanpath
Gaze can be characterized macroscopically by two unique states: fixation, and saccade [12]. Visual information is extracted during fixations, which are periods of relatively small angular movement of the eye. Transitions between fixations take place through the rapid eye movements known as a saccades. A scanpath is the trace of eye movements in space and time [3, 6, 7, 11, 19]. It is a locus of fixation points (x, y, t) which describe when and where the subject attends to a particular visual stimulus. Each scanpath is a distillation of true eye movement, which is complex and continuous. The particular choice of presentation of this data varies by the type of analysis. Among these presentations, the most common consists of plotting the x and y coordinates of each fixation point onto an image of the visual stimulus [11]. The duration of the fixation is illustrated using a circle with a diameter proportional to the amount of time. An example scanpath of one subject and one trial is shown in Figure 3.

There are several techniques used to generate the scanpath, each of which depend on the particular method to identify and label fixations and saccades. Many popular methods

are outlined in [23]. The methods can generally be broken down into two main types; area/dispersion based methods which rely on the spatial distribution of the BPOR onto an image of the visual stimulus, and velocity based methods which utilize the angular velocity of the eye. Area/dispersion based methods are widely used in print based studies to compare regions of visual interest, especially in test scenarios in which the subject's head is fixed, or nearly fixed. Velocity based methods analyze the distribution of the angular motion of the eye itself. It is generally accepted that the eyes cannot move faster than a given speed; usually $900°$ per second. It is also generally accepted that saccades are defined by shifts that occur above certain speeds. Furthermore, the human attention system cannot interpret complex visual stimuli lasting for a duration of less than 100-200ms [11]. This makes the velocity based methods more attractive as they can be made to adhere to such physiological constraints. In addition, our subjects are free to move their heads as they chose, making a velocity based method the only viable option.

In order to generate our scanpaths, we extracted fixations from the time history of the BPOR using a methodology outlined in [20]. We have found this method to be flexible enough to work well at our sampling rate of 60 Hz, yet robust enough to extract saccades even in the presence of noise. It estimates a saccade as a peak in the angular velocity of the eye which occurs above a threshold determined from the statistics of the data. These data may have measurement noise from periodic occlusions of the pupil, or more often, may represent eye movements that are naturally more jittery.

Before calculating our scanpaths, we first condition the raw gaze data using a Savitzky-Golay filter to calculate the angular velocities eye $\dot{\theta}$, and remove points with unusually high velocity ($>900°$/sec). These points are most likely due to the inability of the eye tracking system to properly image the pupil. Next, we remove any remaining points located at the origin (as a result of blinks or loss of pupil tracking) and those points located outside the data window. Approximately 1-5% of the BPOR data must be removed for these reasons. Finally, we interpolate between the removed points.

We prime the estimation algorithm by choosing some initial peak velocity threshold $\dot{\theta}_{init}^{PT}$ that is greater than the maximum velocity in the data, and define the set used in the first estimation as $\omega_1 = \{\omega \in \dot{\theta} \mid \omega < \dot{\theta}_{init}^{PT}\}$. Next, the estimation process iterates until the exit threshold is reached (Step 4). The ith iteration is described below.

1. Calculate the mean and standard deviation of ω_i, as μ^{ω_i} and σ^{ω_i}.
2. Define a new peak velocity threshold $\dot{\theta}_{i+1}^{PT} = \mu^{\omega_i} + 6\sigma^{\omega_i}$
3. Define the new set $\omega_{i+1} = \{\omega \in \dot{\theta} \mid \omega < \dot{\theta}_{i+1}^{PT}\}$.
4. If $\mid \dot{\theta}_{i+1}^{PT} - \dot{\theta}_i^{PT} \mid < 1°$/sec, then the final threshold is $\dot{\theta}_F^{PT} = \dot{\theta}_{i+1}^{PT}$ and the angular velocity of the onset and offset as $\dot{\theta}^o = \mu^{\omega_{i+1}} + 3\sigma^{\omega_{i+1}}$, else return to step 1.

Once we have determined the velocity threshold, we extract the peaks in angular velocity data, which is essentially the set that satisfies $\omega_{peak} = \{\omega \in \dot{\theta} \mid \ddot{\theta} = 0\}$. Saccades are defined in the angular velocity data as $\dot{\theta}_{sac} = \{\omega \in \dot{\theta} \mid \omega_{peak} >$

$\dot{\theta}_F^{PT}, \omega_{peak} - \dot{\theta}^o \leq \omega \leq \omega_{peak} + \dot{\theta}^o\}$. Any part of the signal that is not a saccade is categorized as a fixation. Depending upon the subject, approximately 5-8% of fixations are less than 100 ms, and must be discarded. Finally, we calculate the mean value of the position of the eye (in pixels) for each fixation. The resulting vector tuple is the (x, y, t) elements of the fixation.

The objective comparison of scanpaths depends heavily on both the task, and the visual stimulus. A detailed review of many of these comparison methods are outlined in [11]. In our particular study however, the comparison is vastly simplified. We included the vertical marks on the test sample to force a visual engagement with the workpiece. As a result, the scanpaths evolve in a manner analogous to a reading task in which the visual stimuli, the words, are generally examined serially from left to right. We know that a subject is likely to attend to the words on the page and in a specific order. Similarly, since our grinding task is limited to the surface of the small test coupon, we can assume that the subjects are likely to spend the majority of time searching vertically and horizontally. Therefore, the difference in gaze behavior becomes how often, and at what magnitude does their gaze shift across the test sample.

3.3 Process Parameters

In order to determine process parameters for direct comparison of product performance, material removal and average surface roughness were measured. A white light interferometer confocal microscope CSM 700 from Zeiss was used to measure all 2D and 3D surface roughness parameters with a cut-off length of 0.8 mm and an evaluation length of 4 mm (in accordance with ISO 4287:1997). A weighing scale was used to measure mass of workpieces before and after each grinding for each subject.

4 Results and Discussion

In this section, we compare the behavioral characteristics between subjects. We examine the duration of fixations, the variance of fixation positions, the characteristics of the applied forces, and identify general relationships between the eye movement, grinding forces, and tool velocity. We then compare process performance variables (MMR) and part quality (average surface roughness) resulting from the grinding operation. Finally, we discuss how the differences in gaze-sensorimotor behavior, are related to process performance and part quality via technique, which is a crucial element of the experience level of the subject.

As noted earlier, we shall refer to the experienced subject as Subject 1, the intermediates as Subject 2 and Subject 3, and the novice as Subject 4. Furthermore, for the purpose of direction consistency, we will refer to the x direction of the gaze as tangential and the y direction as axial.

4.1 Tool Velocity

For this particular study, the addition of the motion tracking system allowed us to directly measure the position

and orientation of the tool. Figure 2 provides a detail of the Dremel tool with the tracking spheres attached. Velocities were calculated by a simple numeric differentiation of the filtered position measurements. The velocity vector was decomposed into the relevant axes: tangential (x), normal (z), and axial (y) as shown in Figure 2.

In order to directly compare the velocity characteristics of each subject, the absolute value of the signals were binned and normalized. These results are shown in Figure 4. Despite the fact that this grinding task was primarily tangential in nature, several of the subjects displayed interesting variations in their axial motion. A close examination of the curves in Figure 4 shows that Subject 2 and Subject 4 show a large tangential response between .06 to .1 m/s, as we might expect. However, Subjects 1 and 3 have low variance in both the axial and tangential directions indicating that their hand motions contained a fair amount of axial motion. In fact, both of these subjects tended to utilize a swirling motion over the workpiece rather than a standard back and forth sweeping of the tool. These differences in technique are embodied in the remainder of the behavior data.

4.2 Gaze Analysis

Fixation duration is simply measured as the time lapse, in seconds, between two saccades. A two sample t-test and a chi-squared test were performed on the fixation data. These tests both indicate that trials between subjects are statistically different ($p < 0.03$), while the data within each subject are not. This is plausible as we may guess that the fixational characteristics are an inherent property of the individual subjects. As a result, we pooled the data for each subject across all ten trials.

The pooled distributions as illustrated in Figure 5 are highly skewed. A direct comparison between the subjects shows that Subject 1 and Subject 3 have much shorter durations than Subject 2 and Subject 4, which indicates that their eyes are moving about the workpiece more frequently. Furthermore, Subject 1 shows the smallest variance, with few durations lasting longer than 2 seconds. By comparison, Subject 4 has the largest variance of the all subjects with some fixations lasting as long as 4 seconds, more than twice that of Subject 1.

We can invert these fixation duration data in order to obtain a distribution of fixation frequency as shown in Figure 9. This method to effectively display the data for comparison with the spectral distribution of the tangential forces and velocities.

Figure 7 shows the distribution of the gaze variations. A typical set of fixations for a single grinding trial are illustrated in Figure 6. We determine the variations as follows: First, the mean for each trial is calculated. The variation is defined as the square root of the squared difference of the gaze position from the mean for each fixation. Thus it is not the variance of a distribution, but the absolute value of the distance of each fixational point of regard from the mean of each particular trial. These data are presented as pixels in the image frame (1280 horizontal by 960 vertical). These

data are binned and the distribution of each subject for each trial is plotted in Figure 7. Since this particular task is performed by moving the tool from side to side, we would expect that the fixational shifts would be larger in the horizontal (x) direction than the vertical (y). This appears to be true with Subjects 2 and 4, with the novice subject exhibiting the largest horizontal shifts. Interestingly, Subject 1 and Subject 3 both have tendencies to look vertically more than horizontally corresponding to a shifts in attention in that direction. This corresponds to the more complex motions that were exhibited by these subjects.

4.3 Grinding Forces

Figure 8(a) illustrates the normal versus the tangential forces for a single trial of each of the four subjects. While the normal forces might be considered those that are directly applied by the subject, we can see that there is a strong correlation between the tangential and normal forces (r^2 between .65 and 0.85 for all subjects). However, the tangential force is also an indication of the grinding power as the greater the magnitude, the more energy involved in the material removal [21] and therefore more relevant to process performance. Finally, the variability in the distributions of the tangential forces between subjects were large enough to analyze statistically. Therefore, we chose to include the tangential rather than normal forces in our comparative analysis.

While the different subjects operated in different force regimes, it is clear from Figure 8 that the mean value of the forces produced by Subject 2 were the highest, while those from Subject 1 were the lowest. More importantly however, the mean and variance in both the normal and tangential forces for both Subject 2 and Subject 4 are very large compared to the others, indicated a general tendency to push the tool harder into the workpiece.

4.4 Relationship Between Gaze, Tool Velocity, and Applied Forces

In this section, we examine the relationships between a subject's shifts in gaze and the corresponding changes in applied force and tool velocity. Our experimental setup cannot measure where in space a force was applied, only its components along the principle axes of the triaxial load cell. However, we can track how the tangential forces change, and correspondingly, how the eye movements and tool positions change in the same direction.

As a means of comparing the frequency characteristics of the gaze, tangential force, and the axial and tangential velocity properties of each subject, we have overlaid the frequency distributions of the fixations and power spectral densities onto a single plot. These plots are shown in Figure 9. We see that collective responses of each of the subjects exhibits a modal shape. These modes arise through the proprioceptive interaction of the human subjects with the natural dynamics of the mechanical system. We cannot say for certain which regime may predominate in this particular frequency band. However, the clamped test article is extremely stiff, and the grinding wheel was rotating at 5000 rpm. Me-

chanical resonances are most likely absent at such frequencies. Therefore it is likely that the force response in the 0 to 10Hz bandwidth is dominated by the characteristics of the gaze-motor system. The modes in these spectra are located at: Subject 1: 3Hz; Subject 2: 2.1Hz; Subject 3: 3.1Hz; Subject 4: 2.5Hz.

These modes encapsulate the behavioral characteristics of the subject as they perform the manual grinding task. It is clear that the peaks tool velocities similarly occur with peaks in tangential forces. These are the applied hand motions and the applied tool forces respectively. Likewise, Subjects 1, 3, and 4 all display a rolloff in their fixational response at frequencies corresponding to the force and velocity peaks. Hand motion and applied force occur together indicating purposeful movement, and similar changes in gaze behavior indicate a shift in attention corresponding to this movement. The coexistence of these modes show that, for this manual grinding task, visual attention is coupled to the motor system in a sensory feedback loop, and that we observe this to be so. The impact of this observation will be discussed in Section 4.6.

Going further, if we refer back to Figures 4-9, the difference in the behavior of each of the subjects becomes more clear. Subject 1 and Subject 3 perform the task in a precise manner by moving the tool in complex paths, both axially and tangentially, with lower applied forces and velocities, and short fixations. By contrast, Subject 2 and Subject 4 move the tool primarily tangentially, with higher tangential forces and longer fixations. There is a clear contrast in the behaviors between these two groups of subjects.

4.5 Relationship Between Applied Force and Surface Integrity

Material removal rate (MMR) or mass removed during a machining operation is a useful parameter to understand cutting mechanisms. Overall, cutting mechanisms can be divided into three phases: rubbing, plowing, and cutting. For low MMR, rubbing and plowing dominates over the chip formation process. Conversely, at high MMR, chip formation dominates. Since energy is lost to heat conversion in the plowing and rubbing phases, higher proportions of chip formation lead to a more effective grinding process. For manual operations, cutting forces applied to the workpiece come from both the cutting tool rotation and worker's manual feed and normal pressure onto the workpiece. Depending on the experience of the user, applied forces can vary over a wide range and affect the consistency of machining process.

Grinding forces are important quantitative process indicators to characterize MRR and specific grinding energy, and are strongly tied to surface damage. Grinding power (P_c) is a function of tangential forces (F_t) and the circumferential tool speed (v_s) and is represented as: $P_c = F_t v_s$. Figure 10 shows the tangential force variation versus mass removed for the different subjects. For an approximately equivalent amount of material removed, the novice subject requires 2.5 times more tangential force than the experienced subject. For the intermediate subjects, Subject 2 and Subject 3, with the ex-

ception of a single outlier for each, the material removed are in ranges similar to that of Subject 1. However, Subject 2 requires a 1.3 and 2 times greater grinding force per equivalent amount of material removed compared to that of Subject 3 and Subject 1 respectively.

The variation of the normal forces shown in Figure 11 are similar to the tangential forces shown in Figure 10. With the exception of the novice subject (Subject 4), all other subjects applied forces in defined force regimes, whereas the novice subject displays inconsistent behavior which might result in unreliable product quality. Similar to Figure 10, for the same amount of material removed, Subject 2 applied higher normal forces compared to the other two subjects. Higher grinding forces create higher temperatures that lead to greater surface wear under dry cutting conditions. Both forces and temperatures influence workpiece quality and accuracy such as surface roughness, force ratio, grinding energy etc. Higher grinding forces also increase the wear rate of the abrasive tool. Therefore, it is desirable to reduce the grinding force during the machining process.

In addition to grinding force, surface roughness is assumed to be another indicator used to characterize the material removal mode associated with the grinding process. The quality of surface generation depends on the material removed during the grinding operation. The average surface roughness produced by the different subjects with respect to material removed is shown in Figure 12. In order to achieve the same amount of average surface roughness, Subject 2 removed less material, with a lower average roughness compared to other users. However, Subject 1 showed higher consistency in terms of material removed, whereas Subject 4 exhibited a wide range over the different trials. Overall, we can conclude that the increase in material removed did not directly affect surface morphology.

Figure 13 shows the relationship between tangential forces and average surface roughness. Figure 13 shows that average values of roughness vary from subject to subject, but display a negative association with tangential force except for Subject 4. Subject 1 applied lower tangential forces compared to the other subjects, but average roughness for 10 trials are higher than others, whereas for Subject 2 applied higher forces which lead to lower roughness generation on the workpiece. Overall, the average surface roughness of Subject 2, 3, and 4 were lower compare to Subject 1. However, in terms of producing reliable product quality, Subject 1 is consistent compared to other users.

These facts led to the conclusion that manual grinding operations are critically dependent on manual feed, and normal forces applied on workpieces to produce reliable product quality and to maintain performance consistency. Unlike automated conventional grinding operations, in manual operations both normal and tangential forces are affected by user's experience rather than material removed.

4.6 Practical Implications and Impact

In our analysis of the individual behaviors, we see that there is a contrast between Subjects 1 and Subject 3 com-

pared to those of Subject 2 and Subject 4. As we discussed in Section 4.4, Subject 1 and Subject 3 utilized more complex tool paths than Subject 2 and Subject 4. We will refer to the class of these behaviors as the exhibition of a technique. For ease of syntax, we will refer to Subject 1 and Subject 3 as using Technique A, and Subject 2 and Subject 4 as using Technique B. The behaviors corresponding to these techniques have been summarized in Table 1 for clarity.

We also examined process parameters and discovered that Subject 1 and Subject 3 are able to remove more mass while utilizing lower tangential, and lower normal forces, indicating a more efficient grinding process. Furthermore, both Subject 1 and Subject 3 have low variation in applied forces and material removed implying a much more consistent process output. While Subject 1 shows larger average surface roughness than the other three subjects, the variation in this from trial to trial is extremely low, again indicating consistency. Of all the subjects, Subject 1 produced a product consistently and efficiently, followed closely by Subject 3. While Subject 2 was both less consistent and efficient, the subject does display characteristics of one who has experience with the grinding tool. By contrast, the performance of Subject 4 is highly random. This subject is able to perform the task, but shows little ability to produce in a repeatable fashion.

We can now summarize the relationships that we have discovered. Technique A was comprised of complex tool paths and low forces. This technique was exhibited by Subject 1 and Subject 3. These subjects also produced a more consistent product, more efficiently. Technique B, which included simple tangential tool paths and higher grinding forces was exhibited by Subject 2 and Subject 4. It resulted in a less consistent and less efficient output. Therefore, we have observed a relationship between manual grinding techniques which are displayed by practitioners of different levels of experience. The sensorimotor behaviors embedded in these techniques are observable and distinguishable. Finally, the techniques result in in different product outputs observed in the process parameters.

In order to digitalized human performance, we would like to be able to join the behavioral and process parameter properties together in a formal model. The findings from this pilot study show that this may be viable. Certainly an experiment with a larger cohort of subjects representing each experience level would be required in future work. A recognition of sensorimotor behaviors and their effects on the process outputs can be used to interrogate the manner in which each subject performs the task beyond their own internal perception. This in turn can be used to inform a personalized teaching regime. Furthermore, the design of a more thorough experiment could examine the eye and hand movements for a wider range of tasks (possibly two dimensional grinding) and how the forces and velocities change between "important" saccades. The possible rule for quantifying the importance of a saccade can be a function of the experience of the practitioner.

5 Conclusion

Our long term goal is to develop a principled and data-driven way of analyzing human manual skills. Since the skills involved in complex manual tasks need the close integration of multiple processes, a difficulty in the analysis lies in how to deal with data collected from processes of a different nature. Yet this is critical if we wish to join behavioral and process parameter properties together in a formal model. Finding the right balance between process parameters and product performance is important for maximizing process efficiency.

In this paper, we have examined the visual-attention-motor behavioral characteristics involved in a manual grinding task. Four subjects of various experience levels were used in this pilot study. We were able to show that there were observable and distinguishable sensorimotor behaviors associated with two distinct techniques utilized by the individual subjects, and that task performance is effected by these techniques. Different cutting forces, and tool velocity are some of the very critical factors among a vast amount of other considerations, which have a direct impact on machined surface quality and material removal. Unlike automated processes, we see that in manual operations a user's skillset influences the process performance and consistency. Moreover, we can distinguish between the behavioral characteristics associated with observed techniques which can aid in digitalization of manual performance and inform personalized training regimes. In our future work, we will continue to analyze product performance associated with processing parameters and the unique behaviors of the operators.

6 Acknowledgment

References

[1] Gregory Bales, Jayanti Das, Barbara Linke, and Zhaodan Kong. Recognizing Gaze-Motor Behavioral Patterns in Manual Grinding Tasks. *Procedia Manufacturing*, 5:106–121, 2016.

[2] Ali Borji and Laurent Itti. State-of-the-art in visual attention modeling. *Pattern Analysis and Machine Intelligence, IEEE Transactions on*, 35(1):185–207, 2013.

[3] Filipe Cristino, Sebastiaan Mathôt, Jan Theeuwes, and Iain D Gilchrist. Scanmatch: A novel method for comparing fixation sequences. *Behavior research methods*, 42(3):692–700, 2010.

[4] Jayanti Das and Barbara Linke. Effect of Manual Grinding Operations on Surface Integrity. *Procedia CIRP*, 45:95–98, 2016.

[5] Jayanti Das and Barbara Linke. Evaluation and systematic selection of significant multi-scale surface roughness parameters (SRPs) as process monitoring index. *Journal of Materials Processing Technology*, January 2017.

[6] Andrew Duchowski. *Eye tracking methodology: Theory and practice*, volume 373. Springer Science & Business Media, 2007.

[7] Andrew T Duchowski, Jason Driver, Sheriff Jolaoso, William Tan, Beverly N Ramey, and Ami Robbins. Scanpath comparison revisited. In *Proceedings of the 2010 Symposium on Eye-Tracking Research & Applications*, pages 219–226. ACM, 2010.

[8] Tom Erez, Julian J Tramper, William D Smart, and Stan CAM Gielen. A pomdp model of eye-hand coordination. In *AAAI*, 2011.

[9] E. Francalanza, J. Borg, and C. Constantinescu. Development and evaluation of a knowledge-based decision-making approach for designing changeable manufacturing systems. *CIRP Journal of Manufacturing Science and Technology*, 16:81–101, January 2017.

[10] E Goldstein. *Cognitive psychology: Connecting mind, research and everyday experience*. Cengage Learning, 2014.

[11] Kenneth Holmqvist, Marcus Nyström, Richard Andersson, Richard Dewhurst, Halszka Jarodzka, and Joost Van de Weijer. *Eye tracking: A comprehensive guide to methods and measures*. Oxford University Press, 2011.

[12] Alan Kennedy. Eye tracking: A comprehensive guide to methods and measures, 2016.

[13] A. Khellouki, J. Rech, and H. Zahouani. The effect of abrasive grain's wear and contact conditions on surface texture in belt finishing. *Wear*, 263(1-6):81–87, September 2007.

[14] Zhaodan Kong and Bérénice Mettler. Modeling human guidance behavior based on patterns in agent–environment interactions. *Human-Machine Systems, IEEE Transactions on*, 43(4):371–384, 2013.

[15] Michael F Land. Vision, eye movements, and natural behavior. *Visual neuroscience*, 26(01):51–62, 2009.

[16] Jay Lee, Behrad Bagheri, and Hung-An Kao. A Cyber-Physical Systems architecture for Industry 4.0-based manufacturing systems. *Manufacturing Letters*, 3:18–23, January 2015.

[17] Bérénice Mettler, Zhaodan Kong, Bin Li, and Jonathan Andersh. Systems view on spatial planning and perception based on invariants in agent-environment dynamics. *Frontiers in neuroscience*, 8, 2014.

[18] S. Mezghani and M. El Mansori. Abrasiveness properties assessment of coated abrasives for precision belt grinding. *Surface and Coatings Technology*, 203(5-7):786–789, December 2008.

[19] David Noton and Lawrence Stark. Scanpaths in saccadic eye movements while viewing and recognizing patterns. *Vision research*, 11(9):929–IN8, 1971.

[20] Marcus Nyström and Kenneth Holmqvist. An adaptive algorithm for fixation, saccade, and glissade detection in eyetracking data. *Behavior Research Methods*, 42(1):188–204, February 2010.

[21] Kyle Odum, Maria Celeste Castillo, Jayanti Das, and Barbara Linke. Sustainability analysis of grinding with power tools. *Procedia CIRP*, 14:570–574, 2014.

[22] Michael I Posner. *Cognitive neuroscience of attention*. Guilford Press, 2011.

[23] Dario D Salvucci and Joseph H Goldberg. Identifying fixations and saccades in eye-tracking protocols. In *Proceedings of the 2000 symposium on Eye tracking research & applications*, pages 71–78. ACM, 2000.

[24] Nathan Sprague, Dana Ballard, and Al Robinson. Modeling embodied visual behaviors. *ACM Transactions on Applied Perception (TAP)*, 4(2):11, 2007.

[25] Lihui Wang, Martin Törngren, and Mauro Onori. Current status and advancement of cyber-physical systems in manufacturing. *Journal of Manufacturing Systems*, 37:517–527, October 2015.

[26] Tytus Wojtara, Masafumi Uchihara, Hideyuki Murayama, Shingo Shimoda, Satoshi Sakai, Hideo Fujimoto, and Hidenori Kimura. Human–robot collaboration in precise positioning of a three-dimensional object. *Automatica*, 45(2):333–342, 2009.

[27] Weilie Yi and Dana Ballard. Recognizing behavior in hand-eye coordination patterns. *International Journal of Humanoid Robotics*, 6(03):337–359, 2009.

List of Figures

List of Tables

Table 1.   Summary of behaviors exhibited between techniques

	Technique A	**Technique B**
Tool Velocity	greater axial	less axial
Gaze Frequency	more often	less often
Gaze Shifts	more axial	more tangential
Tangential Grinding Force	lower	higher

	Technique	
	A	B
Tool Velocity	sdf	sdf
Gaze Frequency	sfd	fds
Gaze Shifts	fds	fds
Tangential Grinding Force	fsd	fds
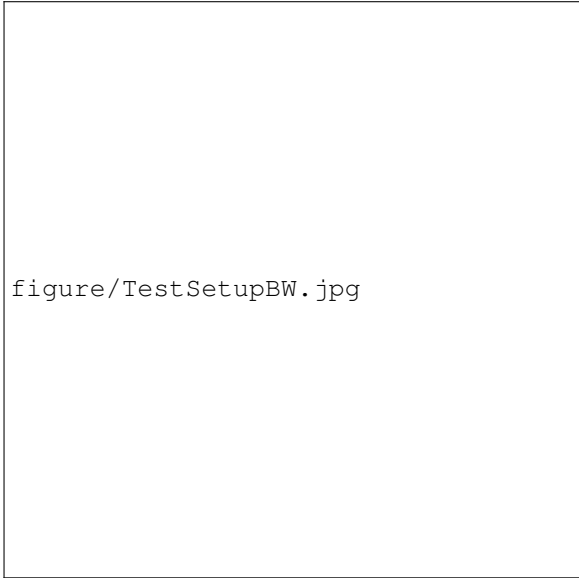
Fig. 1. Setup of our grinding experiment. While the subject was grinding the metal sample, data were collected from three modules: 1) a gaze tracking module, consisting a pair of SMI eye-tracking glasses and a computer running BeGaze data recording software, 2) a force measuring module, consisting of a force sensor and a computer running LabVIEW, 3) an Optitrack motion capture system running Motive, which can determine the position and orientation of selected objects. The data collected from the three modules were synchronized and then analyzed using the methods described in Section 3.
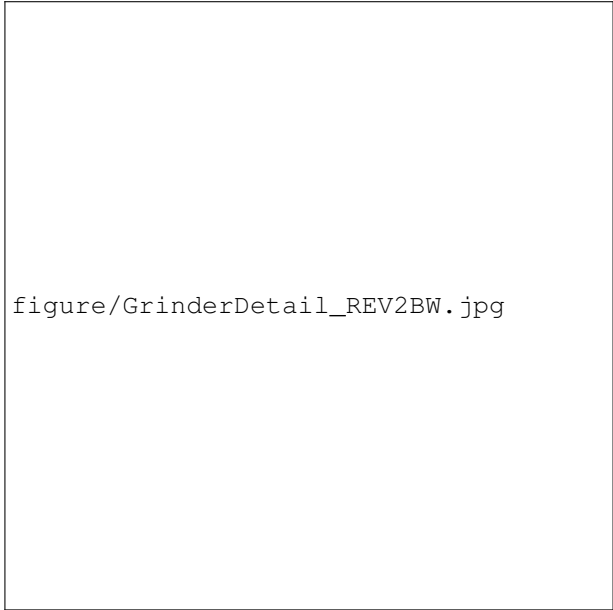
Fig. 2. An image of a grinding sample (left) and a figure showing the force data collection module. Forces in three directions were measured, tangential (x-axis), normal (z-axis) and axial (y-axis). The reflective spheres are used by the motion tracking system.
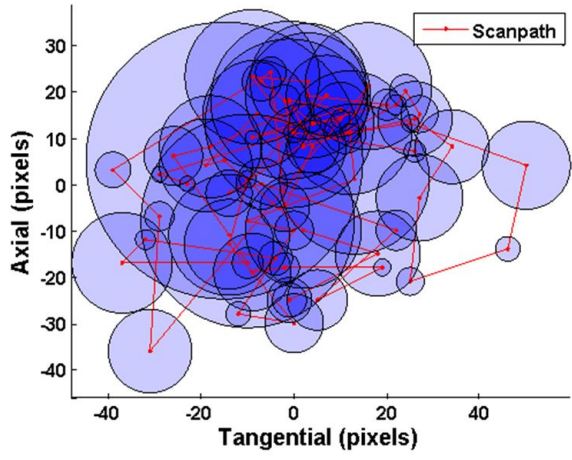
Fig. 3. An example scanpath. The centers of fixations are denoted by points. The durations of fixations are represented by the diameters of the circles. The fixation centers are connected by straight lines according to their temporal order. Each straight line corresponds to a saccade.
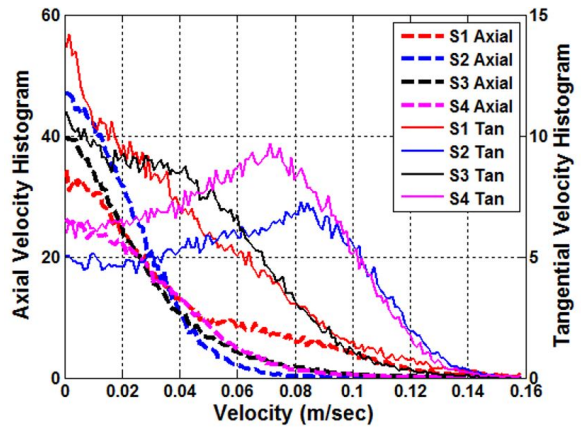
Fig. 4. Normalized histogram of the tangential and axial tool velocities for all subjects
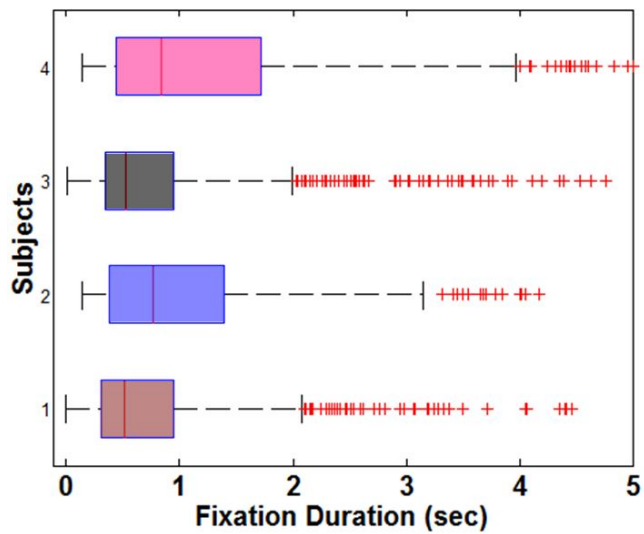
Fig. 5. Comparison of skewed fixation distributions between subjects. Data from all trials for each subject is pooled. Red lines indicate the median of the distribution. Whiskers extend out to the 90th percentiles. Outliers beyond the 90th percentile labeled with a red cross.
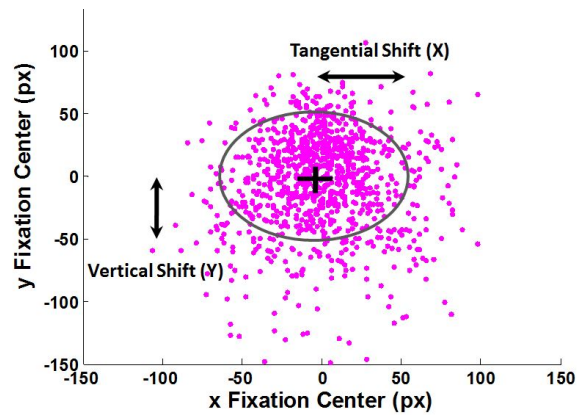
Fig. 6. Sample of fixation points for a single subject. Positions are reported in pixels on the original 1280 by 960 pixel field of view. Notice the asymmetric dispersion of shifts.
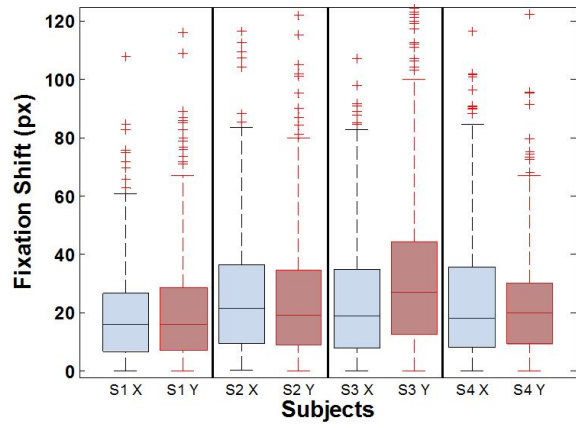
Fig. 7. Distributions of the fixational variations for all the trials. The whiskers extend to the 90th percentile of the distribution. Outliers are represented as red crosses.
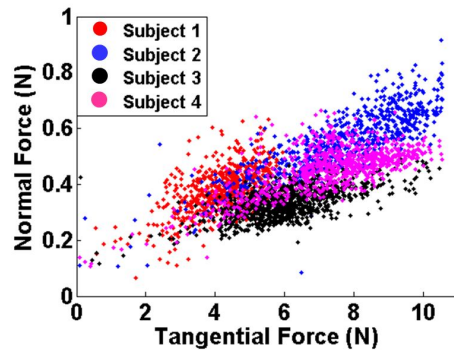
(a)
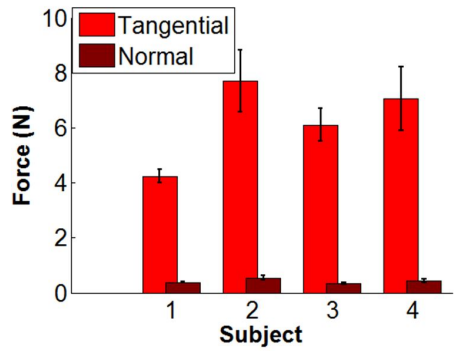
(b)

Fig. 8. (a) Plot of normal and tangential forces for all subjects. (b) Tangential and normal force distributions between subjects. The height of the bars represent the mean force for each trial with the standard deviations indicated.
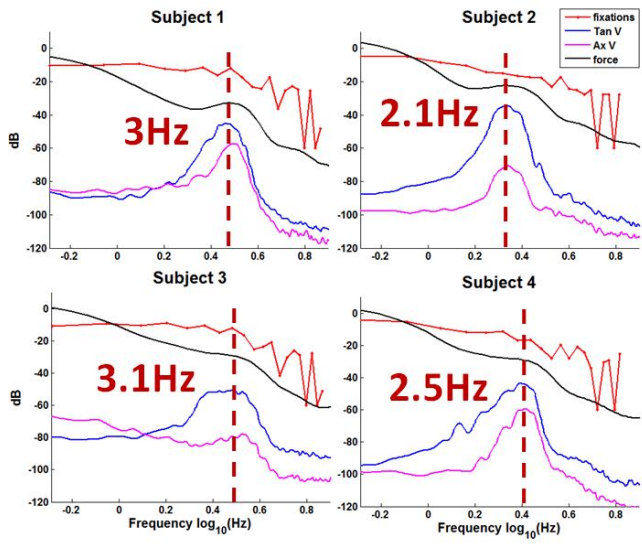
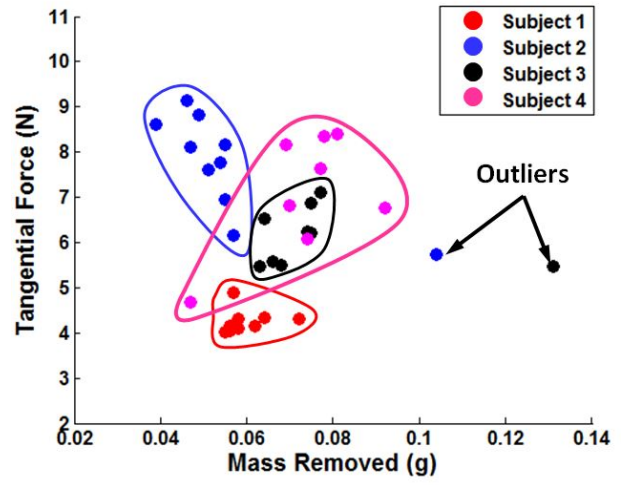Fig. 9.   Comparison of modal responses in the gaze-motor behavior of all subjects

Fig. 10.   Tangential force variation for mass removal during grinding
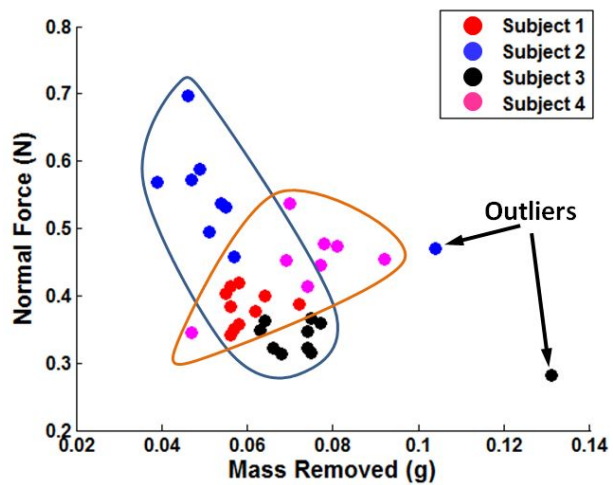
Fig. 11.   Normal force variation for mass removal during grinding
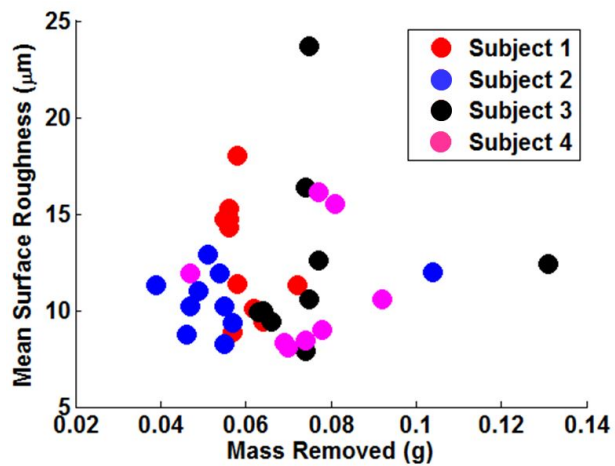

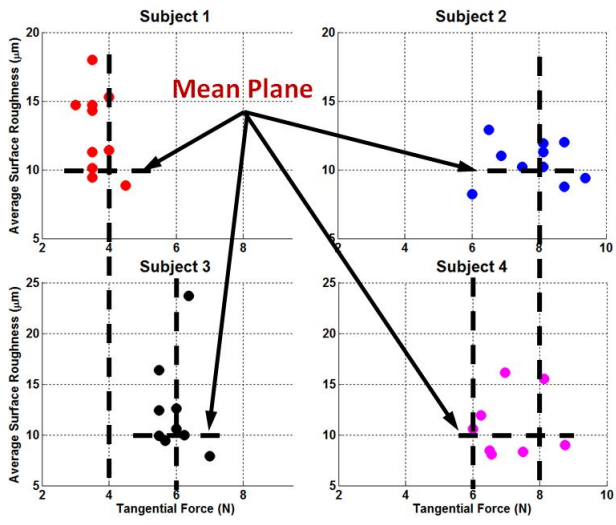Fig. 12.   Mean roughness variation over material removal rate during grinding

Fig. 13.   Mean surface roughness variation with tangential force